

# Optical bistability and multistability via multi-Raman-channel interference

Hongju Guo (郭洪菊)<sup>1,2</sup>, Lichun Wang (汪丽春)<sup>1,2</sup>, Yueping Niu (纽月萍)<sup>1</sup>,  
Shiqi Jin (金石琦)<sup>1\*</sup>, and Shangqing Gong (龚尚庆)<sup>1</sup>

<sup>1</sup>State Key Laboratory of High Field Laser Physics, Shanghai Institute of Optics and Fine Mechanics,  
Chinese Academy of Sciences, Shanghai 201800, China

<sup>2</sup>Graduate University of Chinese Academy of Sciences, Beijing 100049, China

\*E-mail: sqjin@mail.shcnc.ac.cn

Received November 14, 2008

We investigate the optical bistability and multistability behaviors in a closed three-level  $\Lambda$ -type atomic system. By adding a sideband on either hand of the transitions which are originally coupled by a coherent control field and a coherent probe field to disturb the two-photon resonance, bistability occurs due to two-channel interference. Increasing the sideband Rabi frequency leads to the switching from bistability to tristability. When the sideband simultaneously couples with both hands, we can easily obtain quadrastability.

OCIS codes: 020.1670, 190.1450.  
doi: 10.3788/COL20090708.0659.

Quantum coherence and interference in multi-level atomic systems can lead to many interesting optical phenomena<sup>[1–5]</sup> such as lasing without population inversion, enhancement of index, electromagnetically induced transparency (EIT), subluminal and superluminal light. As a role of atomic coherence and interference, optical bistability has been extensively studied both experimentally and theoretically in the past years<sup>[6,7]</sup>. Harshawardhan *et al.* demonstrated the application of EIT and quantum interference effects in the cooperative phenomena of optical bistability<sup>[8]</sup>. Phase fluctuation of the driving field can significantly influence the optical properties of driven atomic systems<sup>[9]</sup>. Utilizing narrow nonabsorption resonances which occurs in a coherently driven three-level system, a bistable behavior can be observed<sup>[10]</sup>. Joshi *et al.* have experimentally demonstrated that the enhanced nonlinearity induced by atomic coherence effects in  $\Lambda$ -type atomic systems can produce the optical bistability and multistability<sup>[11,12]</sup>. Due to the spontaneously generated coherence, the optical bistability can be realized in a nearly equispaced ladder-type three-level atomic system<sup>[13]</sup>. Moreover, Hu *et al.* used trichromatic electromagnetic-field to couple with one transition of the  $\Lambda$ -type atom and thereby induced bistability and multistability<sup>[14]</sup>.

In recent years, Harada *et al.* demonstrated experimentally that stimulated Raman scattering can disrupt EIT<sup>[15]</sup>. The disruption of EIT is important to understand because it may degrade the performance of EIT-based applications, such as optical memories and buffers, and magnetometers. Novikava *et al.* reported a dynamic hysteresis of the Raman scattered optical field in response to changes of the driving laser field intensity and frequency that may be described as a dynamic form of optical bistability<sup>[16]</sup>. Inspired by these studies, in this letter, we add a sideband field on either hand of the atomic transitions to disrupt EIT and obtain bistability due to the two-Raman-channel interference effect. Here

we begin with a two-photon resonance system and then prepare another Raman channel to interfere, and find that only one sideband is enough to give rise to bistability. When we increase the sideband Rabi frequency, bistability is switched to tristability. When a sideband simultaneously couples with both transitions, two  $\Lambda$ -type two-photon resonance Raman channels interfere with each other and quadrastability is easily obtained.

The  $\Lambda$ -type system we consider here is shown in Fig. 1(a), which consists of an excited state and two lower states, denoted by  $|3\rangle$ ,  $|2\rangle$ , and  $|1\rangle$ , respectively. A control field  $\mathbf{E}_c e^{-i\omega_c t} + c.c.$  and its sideband field  $\mathbf{E}_1 e^{-i(\omega_c - \delta)t} + c.c.$  are applied to the  $|2\rangle \leftrightarrow |3\rangle$  transition. Meanwhile, a probe field  $\mathbf{E}_p e^{-i\omega_p t} + c.c.$  and its sideband (another control field)  $\mathbf{E}_2 e^{-i(\omega_p - \delta)t} + c.c.$  are coupled to  $|1\rangle \leftrightarrow |3\rangle$  transition. For these fields,  $\mathbf{E}_i$  ( $i=c, 1, 2$ , and  $p$ ) are the amplitudes of various field components;  $\omega_c$ ,  $\omega_c - \delta$ ,  $\omega_p$ , and  $\omega_p - \delta$  are the corresponding frequencies;  $\delta$  is the frequency difference between the sideband and the control or

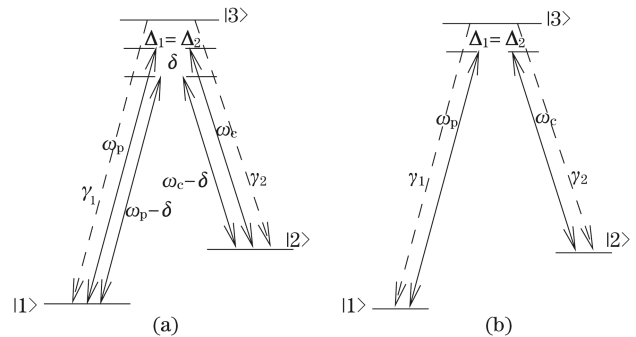


Fig. 1. (a) Three-level  $\Lambda$ -type atom interacting with two coherent fields  $\omega_p$  (the probe field) and  $\omega_c$  (the control field), and two sideband control fields ( $\omega_c - \delta$  and  $\omega_p - \delta$ ) respectively coupling with two transitions.  $\gamma_1$  and  $\gamma_2$  are the atomic decay rates. (b) Three-level  $\Lambda$ -type atom interacting with  $\omega_p$  and  $\omega_c$ .

probe field. A three-level  $\Lambda$ -type system interacting with a control field and a probe field is shown in Fig. 1(b). In Fig. 1,  $\Delta_1 = \omega_{31} - \omega_p$  and  $\Delta_2 = \omega_{32} - \omega_c$  are the detunings of the probe field and the control field from the corresponding transitions,  $\gamma_1$  and  $\gamma_2$  are the atomic decay rates.  $\Omega_i = \frac{\vec{\mu}_{23} \cdot \mathbf{E}_i}{\hbar}$  ( $i=c, 1$ ), and  $\Omega_j = \frac{\vec{\mu}_{13} \cdot \mathbf{E}_j}{\hbar}$  ( $j=p, 2$ ) denote Rabi frequencies associated with the respective fields, in which  $\vec{\mu}_{23}$  and  $\vec{\mu}_{13}$  are the atomic transition electric dipole moments. Under the dipole interaction and rotating wave approximation, the density matrix equations are

$$\begin{aligned}
\dot{\rho}_{33} &= -(\gamma_1 + \gamma_2)\rho_{33} - \frac{i\Omega_p}{2}(\rho_{31} - \rho_{13}) \\
&\quad - \frac{i\Omega_2}{2}(\rho_{31}e^{-i\delta t} - \rho_{13}e^{i\delta t}) - \frac{i\Omega_c}{2}(\rho_{32} - \rho_{23}) \\
&\quad - \frac{i\Omega_1}{2}(\rho_{32}e^{-i\delta t} - \rho_{23}e^{i\delta t}), \\
\dot{\rho}_{11} &= \gamma_1\rho_{33} - \frac{i\Omega_p}{2}(\rho_{13} \\
&\quad - \rho_{31}) - \frac{i\Omega_2}{2}(\rho_{13}e^{i\delta t} - \rho_{31}e^{-i\delta t}), \\
\dot{\rho}_{31} &= -\left(\frac{\gamma_1 + \gamma_2}{2} + i\Delta_1\right)\rho_{31} \\
&\quad - \frac{i(\Omega_p + \Omega_2e^{i\delta t})}{2}(\rho_{33} - \rho_{11}) \\
&\quad + \frac{i(\Omega_c + \Omega_1e^{i\delta t})}{2}\rho_{21}, \\
\dot{\rho}_{32} &= -\left(\frac{\gamma_1 + \gamma_2}{2} + i\Delta_2\right)\rho_{32} + \frac{i(\Omega_p + \Omega_2e^{i\delta t})}{2}\rho_{12} \\
&\quad - i(\Omega_c + \Omega_1e^{i\delta t})\rho_{33} - \frac{i(\Omega_c + \Omega_1e^{i\delta t})}{2}\rho_{11} \\
&\quad + \frac{i(\Omega_c + \Omega_1e^{i\delta t})}{2}, \\
\dot{\rho}_{21} &= i(\Delta_2 - \Delta_1)\rho_{21} - \frac{i(\Omega_p + \Omega_2e^{i\delta t})}{2}\rho_{23} \\
&\quad + \frac{i(\Omega_c + \Omega_1e^{-i\delta t})}{2}\rho_{31}.
\end{aligned} \tag{1}$$

The above equations are constrained by  $\rho_{00} + \rho_{11} + \rho_{22} = 1$  and  $\rho_{ij}^* = \rho_{ji}$ . Expanding  $\rho_{ij}$  as  $\rho_{ij} = \sum_{l=-\infty}^{l=\infty} \rho_{ij}^{(l)} e^{-il\delta t}$  ( $i, j=1, 2, 3$ ) and using matrix inversion technique<sup>[17]</sup>, the steady-state solutions  $\rho_{ij}^{(l)}$  ( $i, j=1, 2, 3$ ) can be obtained.

In what follows, we put the ensemble of  $N$  homogeneously broadened  $\Lambda$ -type atoms in a unidirectional ring cavity (see Fig. 2). For simplicity, we assume that mirrors M3 and M4 have 100% reflectivity, and the intensity reflection and transmission coefficient of mirrors M1 and M2 are  $R$  and  $T$  (with  $R+T=1$ ), respectively.

The Maxwell's equation under slowly varying envelope approximation is<sup>[18]</sup>

$$\frac{\partial E_p}{\partial t} + c \frac{\partial E_p}{\partial z} = i \frac{\omega_p}{2\epsilon_0} P(\omega_p), \tag{2}$$

where  $c$  is the light velocity in vacuum,  $P(\omega_p)$  is the slowly oscillating term of the induced polarization in the

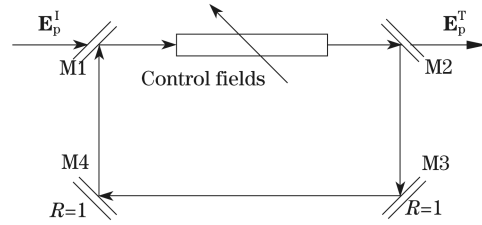


Fig. 2. Unidirectional ring cavity with an atomic sample of length  $L$ , whose configuration is shown in Fig. 1(a).  $\mathbf{E}_p^I$  and  $\mathbf{E}_p^T$  are the incident and transmitted fields, respectively. The control fields  $\mathbf{E}_c$ ,  $\mathbf{E}_1$ , and  $\mathbf{E}_2$  do not circulate in the cavity.

transition  $|1\rangle \leftrightarrow |3\rangle$  and is given by

$$P(\omega_p) = N\mu_{13}\rho_{31}^{(0)}, \tag{3}$$

where  $\rho_{31}^{(0)}$  is the steady-state solution of Eq. (1) which corresponds to the term oscillating at frequency  $\omega_p$ .

Considering the field in the steady-state and setting the time derivative in Eq. (2) to zero, we can obtain the field amplitude as

$$\frac{\partial E_p}{\partial z} = i \frac{N\omega_p\mu_{13}\rho_{31}^{(0)}}{2c\epsilon_0}. \tag{4}$$

For a perfectly tuned cavity, in the steady-state limit, the boundary conditions between the incident field  $E_p^I$  and the transmitted field  $E_p^T$  are

$$E_p(L) = E_p^T/\sqrt{T}, \tag{5}$$

$$E_p(0) = \sqrt{T}E_p^I + RE_p(L), \tag{6}$$

where  $L$  is the length of the the atomic sample. The second term on the right-hand side of Eq. (6) describes a feedback mechanism due to the mirror, which is essential to give rise to bistability, namely, there will be no bistability if  $R = 0$ .

In the mean-field limit, using the boundary conditions and normalizing the fields by setting  $y = \mu_{13}E_p^I/(\hbar\sqrt{T})$ ,  $x = \mu_{13}E_p^T/(\hbar\sqrt{T})$ , we can get the input-output relationship as

$$y = x + C\gamma_1\text{Im}(\rho_{31}^{(0)}) - iC\gamma_1\text{Re}(\rho_{31}^{(0)}), \tag{7}$$

where  $C = \alpha L/2T$  is the cooperation parameter, and  $\alpha = 4\pi\omega_p\mu_{13}^2/\hbar c\gamma_1$ . The second and third terms on the right-hand side of Eq. (7) are vital for the occurrence of bistability.

In the following, we choose the parameters to be dimensionless units by scaling with  $\gamma$  and let  $\gamma = 1$  to evolve numerical calculations.

It is easy to see from Eqs. (1) and (7) that the input-output relationship is determined by the atomic decay rates  $\gamma_1$  and  $\gamma_2$ , the cooperation parameter  $C$ , Rabi frequencies ( $\Omega_c$ ,  $\Omega_1$ ,  $\Omega_2$ ), and frequency detunings ( $\delta$ ,  $\Delta_1$ ,  $\Delta_2$ ). We consider here  $C = 2000$ ,  $\gamma_1 = \gamma_2 = 1$ ,  $\Delta_1 = \Delta_2$ , and plot input-output curves for different parameter values in Figs. 3 and 4. In the absence of sidebands, for the situation  $\Delta_1 = \Delta_2$ , the detunings of the probe and control fields from corresponding atomic transitions are equal. Thus two-photon resonance will result in the trapping of the atoms in the dark state and EIT, namely,

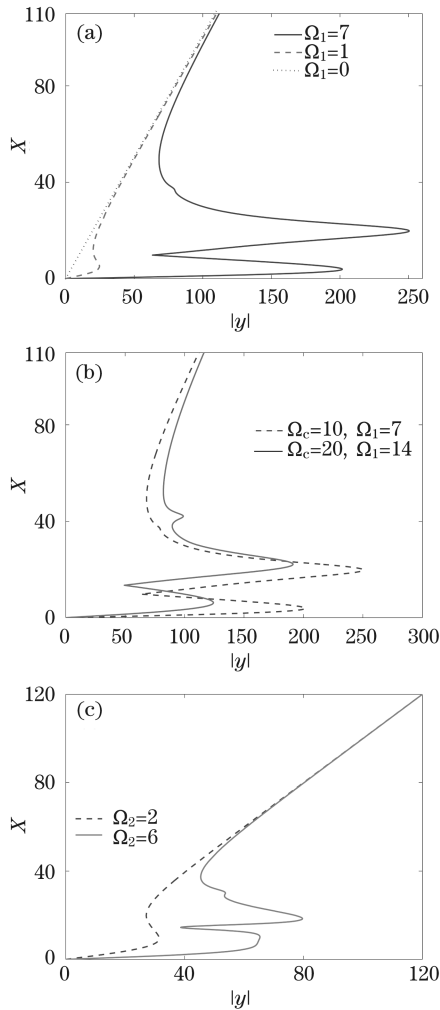


Fig. 3. Input-output relation. (a) Dotted, dashed, and solid lines respectively correspond to  $\Omega_1 = 0, 1,$  and  $7$ . Other parameters are  $\delta = 5, \Delta_1 = \Delta_2 = 0, \Omega_c = 10, \Omega_2 = 0$ . (b) Dashed and solid lines respectively correspond to  $\Omega_c = 10, \Omega_1 = 7$  and  $\Omega_c = 20, \Omega_1 = 14$ . Other parameters are same as those in (a). (c) Dashed and solid lines respectively correspond to  $\Omega_2 = 2$  and  $6$ . Other parameters are  $\delta = -5, \Delta_1 = \Delta_2 = 5, \Omega_c = 10, \Omega_1 = 0$ .

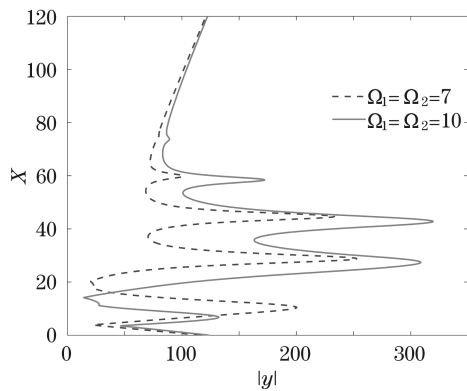


Fig. 4. Input-output relation for parameters  $\Omega_1 = \Omega_2 = 7$  (dashed line),  $\Omega_1 = \Omega_2 = 10$  (solid line) and  $\delta = -5, \Delta_1 = \Delta_2 = 5, \Omega_c = 10$ .

$\text{Im}(\rho_{31}^{(0)}) = \text{Re}(\rho_{31}^{(0)}) = 0$ . It is seen from Eq. (7) that the input-output relation is linear and bistability is impos-

ible, as shown in Fig. 3(a).

Then we apply a sideband on one of the atomic transitions and focus on the behavior of bistability due to two-channel interference effect spoiling EIT. Firstly, setting detunings  $\Delta_1 = \Delta_2 = 0$ , the control Rabi frequencies  $\Omega_c = 10, \Omega_2 = 0$ , and the difference of the sideband  $E_1$  from the control field  $\delta = 5$ , we plot the transmitted light versus incident light for the different sideband Rabi frequencies  $\Omega_1 = 1$  and  $7$  in Fig. 3(a), i.e., the sideband is added to couple with the transition  $|2\rangle \leftrightarrow |3\rangle$ . It is seen that the appearance of the sideband ( $\Omega_1 = 1$  in comparison with  $\Omega_1 = 0$ ) disturbs the two-photon resonance and induces bistability. Moreover, increasing the sideband Rabi frequency from  $1$  to  $7$  induces optical tristability. That means, changing the sideband Rabi frequency can lead to switching from bistability to tristability. In Fig. 3(b), simultaneously increasing the control Rabi frequency and the sideband Rabi frequency from  $\Omega_c = 10$  and  $\Omega_1 = 7$  to  $\Omega_c = 20$  and  $\Omega_1 = 14$ , we can see that the threshold intensity of hysteresis cycle is obviously decreased. Secondly, applying a sideband to the other transition  $|1\rangle \leftrightarrow |3\rangle$  and setting  $\Delta_1 = \Delta_2 = 5$ , the control Rabi frequencies  $\Omega_c = 10, \Omega_1 = 0$ , the difference of the sideband  $E_2$  from the probe field  $\delta = -5$ , we plot the transmitted light versus incident light for the different sideband Rabi frequencies  $\Omega_2 = 2$  and  $6$  in Fig. 3(c). The similar results as in Fig. 3(a) are obtained that the sideband interferes with the two-photon resonance and induces bistability and tristability. We note that two-photon Raman coupling is responsible for normal EIT in the  $\Lambda$  system which is coupled by a control field and a probe field as shown in Fig. 1(b). There exists only one Raman channel  $|1\rangle_{\omega_p} \leftrightarrow |3\rangle_{\omega_c} |2\rangle$ . EIT is induced if the detunings are equal, i.e.,  $\Delta_1 = \Delta_2$ , and a dark state is created<sup>[19]</sup>. When a sideband is added to couple with either transition, another Raman channel  $|1\rangle_{\omega_p} \leftrightarrow |3\rangle_{\omega_c - \delta} |2\rangle$  or  $|1\rangle_{\omega_p - \delta} \leftrightarrow |3\rangle_{\omega_c} |2\rangle$  is opened and interferes with the original channel  $|1\rangle_{\omega_p} \leftrightarrow |3\rangle_{\omega_c} |2\rangle$ . This destructive interference will suppress the light absorption and EIT. Increasing the sideband intensity gives rise to stronger destructive interference. As a result, bistability and tristability occur.

We also consider the case when both transitions are coupled by a sideband. Setting  $\Delta_1 = \Delta_2 = 5$ , the control Rabi frequency  $\Omega_c = 10$ , the difference of two sidebands from the control and the probe fields  $\delta = -5$ , we plot the input-output relationship for the sideband Rabi frequencies  $\Omega_1 = \Omega_2 = 7$  and  $10$  in Fig. 4. From this figure, we can see that respectively coupling an additional sideband with both transitions can easily give rise to multistability. Increasing the sideband Rabi frequencies from  $\Omega_1 = \Omega_2 = 7$  to  $10$ , we can switch quadrastability to pentastability. At the same time, the threshold intensity is decreased, that is favorable for experimental realization.

In conclusion, we investigate the optical bistability and multistability behaviors in a closed three-level  $\Lambda$ -type atomic system by introducing a sideband on either hand of the transitions which are originally coupled by a coherent control field and a coherent probe field. Increasing the sideband Rabi frequency leads to the switching from bistability to tristability due to two-Raman-channel interference. When the sideband simultaneously couples

with both transitions, quadrastability and pentastability can be obtained favorably.

This work was supported by the National Natural Science Foundation of China (No. 60708008), the Project of Academic Leaders in Shanghai (No. 07XD14030), and the Knowledge Innovation Program of the Chinese Academy of Sciences.

## References

1. G. S. Agarwal, Phys. Rev. Lett. **67**, 980 (1991).
2. S. E. Harris, Phys. Today **50**, (7) 36 (1997).
3. M. O. Scully, Phys. Rev. Lett. **67**, 1855 (1991).
4. C. H. Keitel, Phys. Rev. A **57**, 1412 (1998).
5. H. Li, J. Liu, C. Wang, G. Ni, R. Li, and Z. Xu, Chin. Opt. Lett. **5**, S129 (2007).
6. A. Joshi and M. Xiao, Phys. Rev. Lett. **91**, 143904 (2003).
7. L. A. Lugiato. "Theory of optical bistability" in *Progress in Optics Vol. 21* E. Wolf, (ed.) (North-Holland, Amsterdam, 1984) p.71, and references therein.
8. W. Harshawardhan and G. S. Agarwal, Phys. Rev. A **53**, 1812 (1996).
9. X.-M. Hu and Z.-Z. Xu, J. Opt. B **3**, 35 (2001).
10. D. F. Walls and P. Zoller, Opt. Commun. **34**, 260 (1980).
11. A. Joshi, A. Brown, H. Wang, and M. Xiao, Phys. Rev. A **67**, 041801(R) (2003).
12. H. Wang, D. Goorskey, and M. Xiao, Phys. Rev. A **65**, 051802(R) (2002).
13. D. Cheng, C. Liu, and S. Gong, Phys. Lett. A **332**, 244 (2004).
14. X. Hu and J. Wang, Phys. Lett. A **365**, 253 (2007).
15. K. Harada, T. Kanbashi, M. Mitsunaga, and K. Motomura, Phys. Rev. A **73**, 013807 (2006).
16. I. Novikava, A. S. Zibrov, D. F. Phillips, A. André, and R. L. Walsworth, Phys. Rev. A **69**, 061802 (R) (2004).
17. X. Hu, G. Cheng, J. Zhou, X. Li, and D. Du, Opt. Commun. **249**, 543 (2005).
18. H. Ma, S. Gong, C. Liu, Z. Sun, and Z. Xu, Opt. Commun. **223**, 97 (2003).
19. J. Zhang, J. Xu, G. Hernandez, X.-M. Hu, and Y. Zhu, Phys. Rev. A **75**, 043810 (2007).